



Contents lists available at SciVerse ScienceDirect

Journal of Marine Systems

journal homepage: www.elsevier.com/locate/jmarsys

High-frequency study of epibenthic megafaunal community dynamics in Barkley Canyon: A multi-disciplinary approach using the NEPTUNE Canada network

Marjolaine Matabos^{a,*}, Alice O.V. Bui^a, Steven Mihály^a, Jacopo Aguzzi^b, S. Kim Juniper^a, R.S. Ajayamohan^a

^a NEPTUNE Canada, University of Victoria, Victoria, British Columbia V8W 2Y2, Canada

^b Instituto de Ciencias del Mar (ICM-CSIC), Paseo Marítimo de la Barceloneta 37-49, 08003 Barcelona, Spain

ARTICLE INFO

Article history:

Received 11 November 2012

Received in revised form 2 April 2013

Accepted 4 May 2013

Available online xxxx

Keywords:

Anoplopoma fimbria
Hippolytidae shrimp
Instrument platforms
Multivariate analysis
Time-series
Submarine canyons
Canada
British Columbia
Barkley Canyon
Latitude 48°18.89'
Longitude –126°03.49'

ABSTRACT

In the deep sea and along the continental slope, benthic observations have often been limited to seasonal or longer time scales, conducted at irregular and intermittent intervals. The recent development of cabled observatories now permits continuous high-frequency studies of the ecology of deep environments, and will bring greater temporal resolution to our understanding of processes that shape benthic communities. Combining high-frequency quantitative biological and environmental data, we studied the epibenthic megafaunal community at 890 m depth in Barkley Canyon off Vancouver Island (BC, Canada) using the NEPTUNE Canada cabled network. A video sweep of the same 5 m² area was recorded every 2 h during the month of December 1–31, 2011 and examined for species composition and behavior. A suite of instruments provided environmental data at the same location allowing us to relate species and community patterns to environmental variables at different temporal scales using time-series analysis (periodogram and wavelet analyses) and multivariate methods (canonical redundancy analysis and the distance-based Moran Eigenvector Map). At the beginning of our study physical conditions in the lower water column were influenced by a preceding period (late November) of high surface winds and waves that generated enhanced currents down to 840 m depth. These currents created a potentially inhospitable environment for hippolytid shrimp explaining their migration into deeper waters. At the same time a shift in hydrographic properties was occurring in bottom waters with the intrusion of slightly colder (4 to 3.3 °C), and saltier (34.3 to 34.4 psu) waters over approximately 10 days. These changes were accompanied by a shift in benthic community composition from one dominated by hippolytid shrimp to one dominated by buccinid snails. The temporal structure detected in the epibenthic megafaunal community coincided with oscillations detected in the ambient currents. These results reveal the importance of continuous sampling at high-frequency over long durations by enhancing our ability to detect species activity patterns and will contribute to the design of studies and experiments to understand the interaction of factors acting at multiple temporal scales in submarine canyons.

© 2013 Elsevier B.V. All rights reserved.

1. Introduction

The continental margin (i.e. ~200–3000 m depth) is the most geologically diverse and complex component of the deep ocean (Levin and Sibuet, 2012; Levin et al., 2010; Ramirez-Llodra et al., 2010). The margin's slopes represent 11% of the deep-sea floor of which only a small fraction has been studied at variable levels of detail (Levin and Sibuet, 2012; Menot et al., 2010). While the sedimented slope is the most extensive habitat, continental margins also include submarine canyons, cold seeps, subduction zones, cold-water coral reefs and oxygen minimum zones (OMZ). They thus contain steep and complex clinal variations in key habitat features such as hydrography, light intensity and spectral quality, as well as in sedimentation rates and ocean current dynamics (see review by Aguzzi and Company, 2010). These variations can result in depth-related zonal

distributions of benthic faunal communities (reviewed in Carney, 2005; Menot et al., 2010).

Few studies have specifically examined the temporal dynamics of continental margin benthos. Basic principles can be derived from a survey of the general deep-sea literature while bearing in mind the particular physical features of continental margins. Deep-sea ecosystems are dynamic at time scales spanning minutes (e.g. biotic interactions) to millions of years (e.g. tectonic processes). At decadal scales, changes in climatic conditions related to cycles such as the El Niño Southern Oscillation (ENSO) or the Pacific Decadal Oscillation (PDO) may cause changes in benthic species abundance (Arntz et al., 2006; Blanchard et al., 2010; Sellanes et al., 2007). Seasonal variations of vertical organic matter flux from the surface ocean play an important role in regulating food availability for benthic communities down to the abyssal plain (Billett et al., 2010; Ruhl and Smith, 2004). Daily, internal tides, inertial waves and the currents they generate can affect the continental margin benthos through modulations of species behavior and activity (see review in Aguzzi et al., 2011; Wagner et al.,

* Corresponding author. Tel.: +1 2504725089; fax: +1 2504725370.

E-mail address: mmatabos@uvic.ca (M. Matabos).

2007). Predator–prey relationships between the benthos and pelagic species performing diel vertical migration can also result in coupling to the day–night cycle (Aguzzi et al., 2011). More stochastic processes such as benthic storms, river discharge peaks and plankton bloom sedimentation events can also affect deep-sea communities, often in unpredictable ways (Papiol et al., 2012; Thistle et al., 1991; Yahel et al., 2008). Because of a lack of continuous and concurrent quantitative biological and environmental data from deep-sea benthic regions, it is difficult to forecast how changes to different environmental factors will impact deep-sea communities.

Most of our knowledge of deep-sea benthic ecosystems has been gained through the use of traditional sampling gear and instruments deployed from oceanographic vessels or from submersibles. Ship-based surveys helped us understand biodiversity and distribution of deep-sea organisms, but our comprehension of processes that shape and change deep-sea benthic communities at high temporal resolutions is still limited (Glover et al., 2010). Typical sampling frequencies (e.g. monthly to annual) limit the observation of deep-sea communities at time scales shorter than seasons. Thiel et al. (1994) recognized these limitations and recommended a suite of *in situ* instrument configurations and packages to help us better understand deep-sea processes. Many of the important recommendations envisioned in Thiel et al. (1994) are now being realized. The recent development of cabled seafloor observatories with real-time communications and ‘unlimited’ power now permits continuous high-resolution studies of the ecology of continental margins and the deep-sea, including the study of species behavior (Doya et al., 2013; Matabos et al., 2011). Cabled observatories are being established or are currently in operation in several areas of the world ocean. Among them, the NEPTUNE Canada (NC) cabled undersea network, off Vancouver Island, has supported continuous multiparametric (including video) observations of benthic fauna and habitat variables at several deep-water sites since May 2010.

One NC community science experiment has been designed to study benthic–pelagic coupling in Barkley Canyon, a mid-slope submarine canyon (800 to 1000 m depth) in the north-east subarctic Pacific. More specifically the Barkley project aims to study sediment transport through the canyon and its influence on benthic communities in comparison with the influence of surface organic matter supply. Submarine canyons can play an important role in the transport of organic matter to the abyss and are potential biodiversity hotspots (Company et al., 2011). Prior to the NC Barkley community science experiment, the benthic communities in this region had received very little attention. During this investigation, we used an *in situ* observation package, which included a video camera and a suite of environmental sensors, to examine high-resolution temporal variations in the epibenthic megafaunal communities at the NC Barkley Canyon site and to explore how different environmental parameters influenced these variations. Our sampling period (December 2011) corresponded to a time when atmospheric surface storms are frequent in the region (Juniper et al., in press; meteorological buoy 46206 at La Perouse bank maintained by Environment Canada). The primary goals of this study were to (1) identify any high frequency periodicity in the activity of the most abundant megafaunal species based on bi-hourly video observations; (2) document high frequency environmental variations (e.g. currents, hydrographic events); and (3) determine the intensity of species-specific responses to periodic vs. stochastic events.

2. Methods

2.1. The NEPTUNE Canada platform in Barkley Canyon

NEPTUNE Canada (www.neptunecanada.ca) is a cabled undersea network, part of the Ocean Networks Canada Observatory (www.oceannetworks.ca). It consists of a shore station in Port Alberni that provides power and communication to 5 main nodes through an 800 km loop of electro-optical cable and encompasses environments

from the near-shore to the Juan de Fuca mid-ocean ridge off the west coast of Vancouver Island (British Columbia, Canada). This study was conducted at the Barkley mid-canyon sites using two benthic platforms connected to the network at 890 m depth (Latitude 48°18.89' N, longitude 129°03.48' W; Fig. 1). For a more detailed description of the site and the Barkley Canyon array, see Juniper et al. (in press).

2.2. Data collection

Data from all instruments are archived and available in near real-time online using Oceans 2.0 software (<http://dmas.uvic.ca>). The camera was on an automated schedule and all videos were also archived through Oceans 2.0 and can be viewed online at <http://dmas.uvic.ca/Seatube>.

2.2.1. Environmental characterization

Temperature (°C), salinity (psu), pressure (dbar), fluorescence (chlorophyll *a* + phaeopigments) and turbidity were acquired by instruments deployed on the mid-canyon's flank benthic platforms at 890 m depth (Table 1). The two platforms were separated by 70 m (Fig. 1). All measurements were made approximately 1.5 m above the seafloor, and each instrument sampled at a rate of one measurement per minute.

A 150 kHz upward facing acoustic Doppler current profiler (ADCP) provided estimates of water column currents (9 m to 250 m above bottom) and a 2 MHz ADCP provided high spatial and temporal resolution (1.43 cm and 10 s) estimates of the benthic boundary layer currents from 10 cm to 150 cm above the seafloor.

Preliminary data analysis (not shown) revealed that camera lighting had an effect on fluorescence and turbidity readings. All fluorescence and turbidity data collected while the camera lights were running were therefore removed from the analyzed data set.

We made an *a priori* assumption that the response time of the benthic megafaunal species would be longer than our environmental sampling frequency. Consequently, for comparisons between environmental variables and observed changes to megafaunal species, we binned our environmental data into hourly averages (based on the 60 min preceding each hour; Matabos et al., 2012).

2.2.2. Faunal data collection

Images were collected using a 470 Line ROS Inspector low light, color camera, equipped with an 18× optical zoom. A pan/tilt unit allowed complete coverage of seafloor (+/− 90° tilt and +/− 180° pan) and light was available on demand from 2 Deep-Sea Power and Light variable intensity lamps. Five minute video sweeps of the seafloor were acquired at the beginning of every even hour (UTC) from December 1st to December 31st 2011 (videos are available at <http://dmas.uvic.ca/SeaTube>). Each sweep consisted of a 360° pan, at a ca. 45-degree angle below the seabed horizon, with a 2-minute stationary phase at the beginning and the end of each sweep. The total observed area was approximately 5 m². Each video was viewed using VLC 2.0.1©, and individual organisms down to 2 cm were counted manually and identified to the lowest taxonomic level possible. Abundances were standardized to 10 m². To minimize artifacts introduced by ‘sampler bias’, only one analyst conducted visual counts. Sediment suspension events, mainly created by abrupt fish movements, were counted and the reduction in visibility qualitatively assessed on a scale from 0 to 4, where 0 indicates no visibility and 4 indicates perfect visibility.

2.3. Data analysis

To embed our study in a broader context and provide a better understanding of environmental conditions at the time of the study, environmental data were analyzed over 3 months from November 1, 2011 to January 31, 2012, a period bracketing our biological observations.

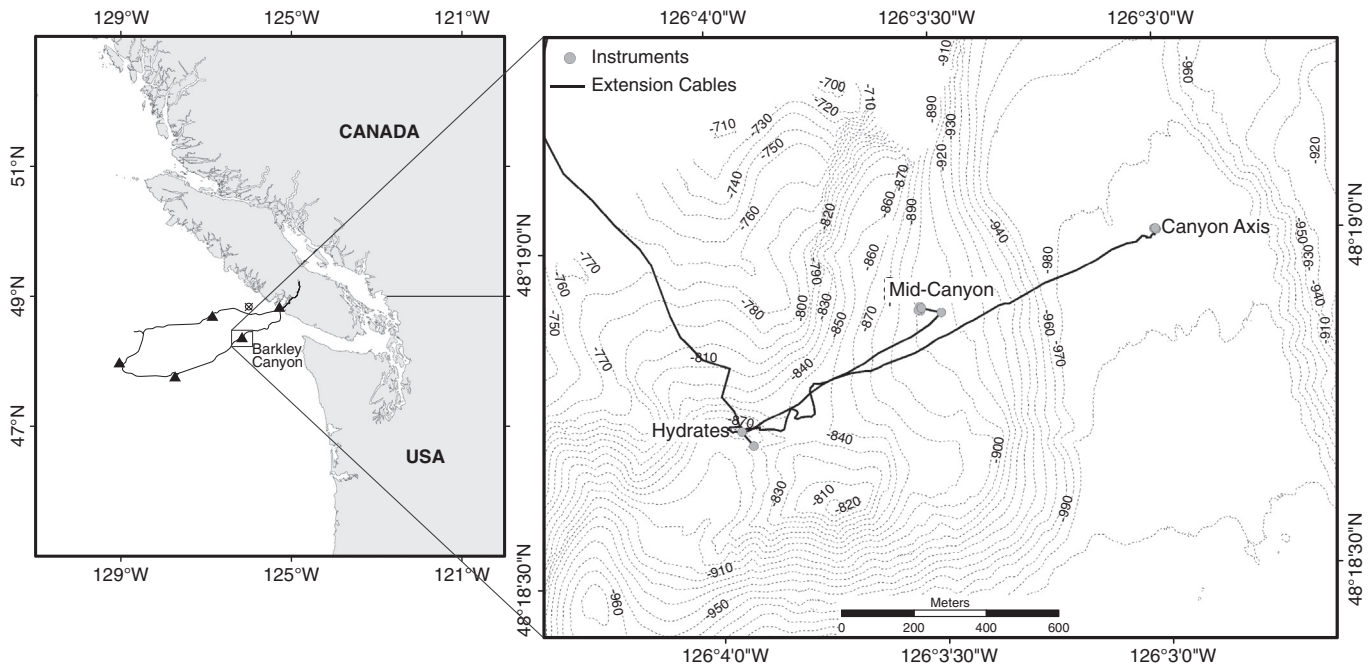


Fig. 1. Location of NEPTUNE Canada camera/instrument site in Barkley Canyon. Left panel shows the NEPTUNE Canada network with the 5 nodes. Crossed circle symbol indicates the location of the meteorological buoy on La Perouse Bank. Right panel illustrates the instruments' pods installation in Barkley Canyon mid-slope. All data used in this study are from pods 3 and 4 at the mid-canyon site.

2.3.1. Water properties and currents

CTD data were processed to remove outliers which were a result of very occasional fouling of the conductivity cell. These data were binned in hourly segments on the hour to be co-temporal with the video data. Bins without sufficient measurements were removed. These hourly data were then low-pass filtered by a 30-h Kaiser-Bessel windowed FIR filter to remove the tidal influence (e.g. Emery and Thomson, 1997). To obtain a representative velocity of near bottom currents we averaged 7 bins centered around 20 cm above the seafloor from the upward facing high resolution ADCP. These data, also smoothed by a Kaiser-Bessel filter to remove the tidal influence, were then averaged over an hourly interval to be co-temporal with the video data. A continuous wavelet transform was applied to the hourly data using the WaveletCo package in the R language (R Core Development Team, 2008) to provide a frequency-time representation of the current field. We based our interpretation primarily on the dominant North-south component, which accounted for 75% of the total variance.

Data from the longer range 150 kHz ADCP were used to quantify the local currents in the water column. To down-sample the large dataset (sampling interval of 1 s), a 15-minute ensemble averaging technique was used. By this method, data were ensemble-averaged into 15-minute bins. A new file was created at the beginning of each day containing 96 × 15-minute interval time segments. A

correlation threshold of 64 and an error velocity threshold of 2 m.s⁻¹ were used to screen the data. Within each bin, only pings that were within these thresholds were used in the ensemble averaging. If there were no good pings, the velocity was marked as a data gap. Data from 15-day segments were concatenated to form a time-series of current data at different depth levels (880 to 640 m).

2.3.2. Biological rhythms

In temporally scheduled imaging studies, variations in visual animal counts can be considered a proxy estimate of the response of local populations to concomitant habitat changes (Aguzzi et al., 2012a). In order to evaluate the presence of diel (i.e. 24-h based) fluctuations in animal abundance of the most abundant species, defined as a species for which we observed more than 2 individuals per day (i.e. sablefish, *Anoplopoma fimbria*; gastropod *Buccinum viridum*; hagfish, *Eptatretus* sp.; hippolytidae shrimp, *Heptacarpus* sp.; squat lobster, *Munidopsis quadrata*; and pelagic shrimps), we divided the full one month time-series into three 10-day sub-segments. Following Sokolove and Bushell (1978), periodogram analyses performed on the three time-series segments screened periodicities from 660 to 1600 min (equal to 11 h and 26 h 42 min, respectively). These periodogram analyses were conducted using the El Temps software (A. Diez-Noguera; University of Barcelona; www.el-temps.com) with the Bonferroni correction and no prior smoothing (e.g. moving average) of input data. In the periodogram output plots, the highest statistically significant (i.e. $p < 0.05$) peak was considered representative of the maximum percentage of total data variance explained by the inherent dominant periodicity. The periodicity was indicated by that peak value and the rhythm strength by the percentage variance (Chiesa et al., 2010).

In order to visualize the occurrence of any progressive modification in population rhythms, waveform analyses were carried out on 10-day time-series fragments (Chiesa et al., 2010). For each 10-day time-series, species counts data were averaged for each 2-h interval in the 24-h day. Significant increments in visual counts (i.e. phase) were determined statistically using the Midline Estimating Statistic of Rhythm (MESOR; Aguzzi et al., 2003). Phase timing and duration were identified by waveform values above the MESOR (i.e. a minimum of three consecutive

Table 1

List of instruments installed on two benthic platforms of the Barkley Canyon wall, and used for the multiparametric data acquisition in this study. Instruments from which the data was not used are not reported.

Site	Instruments	Type	Water property
POD3	ADCP 150 kHz	RDI	Water column currents
	Aquadopp 2 MHz	Nortek	Bottom currents
POD4	Camera system	ROS Inspector	Biology
	Fluorometer	WET Labs ECO FLNTU	Turbidity, chlorophyll <i>a</i> and phaeopigments
	CTD	Sea-Bird SeaCat SBE 16plus	Temperature, salinity, pressure, density

values). MESOR was estimated by re-averaging all waveform values and the resulting value represented as a threshold horizontal line on the waveform plots. In order to establish a cause–effect relationship among bio- and habitat factors, the waveforms for the different species were all represented with superimposed waveform outputs for oceanographic parameters (i.e. water mass density and temperature).

2.3.3. Multivariate analysis

Before conducting multivariate analysis, a Hellinger transformation was applied to the density data (Legendre and Legendre, 1998). This transformation is the square root of the ratio of each species' density to the total density at that observation date. After this transformation, the Euclidean distance is preserved in Euclidean analyses such as canonical redundancy analysis or the distance-based Moran's Eigenvectors Map (dbMEM). Next, the global community was analyzed in relation to environmental factors using a canonical redundancy analysis (RDA). The RDA combines aspects of ordination and regression and uses a permutation procedure to test the significance of the explained variation; thus species abundance data do not need to be normally distributed (Legendre and Legendre, 1998).

A dbMEM was then used to quantitatively describe the temporal structure of the community (Borcard and Legendre, 2002; Peres-Neto and Legendre, 2010). This method was 'borrowed' from spatial ecology where it was used to detect and quantify spatial structures over a wide range of scales encompassed by the sampling design. It has significant advantages over more traditional time-series analysis for ecological time-series; it determines patterns at different scales and identifies which species and environmental variables contribute to those patterns (Angeler et al., 2009). Before applying this method, the species response data were analyzed for linear trends using a RDA between the species data matrix and the time vector and only the detrended data were kept for further analysis. The matrix of Euclidean distances, generated from sampling date time coordinates, was truncated with a threshold of 2, which is the distance between two neighboring sampling times. A principal coordinate analysis applied on the truncated matrix created 271 dbMEMs, and only the 185 with positive Moran's I values were retained. The resulting principal coordinates (dbMEM eigenfunctions) were regular sinusoids describing all temporal scales that could be detected in the sampling design. These variables were then used in an RDA to explain variations in epibenthic megafaunal community composition that were related to temporal structure. A forward selection of the positive dbMEMs, implemented to select a parsimonious model, identified 51 significant dbMEMs that were selected for further analysis. This procedure uses a permutation test (999 random permutations) to examine the significance of the explanatory variables (here the dbMEMs functions) successively entered into the model. It stops when either the p-value of a newly included variable is higher than an alpha threshold of 0.05, or the contribution (adjusted R^2) of a newly entered variable is lower than a threshold equal to the R^2 value from the initial RDA (see above). The 51 significant dbMEMs were grouped visually in sub-models (i.e. time scale) according to their sinusoid periods. A Whittaker–Robinson periodogram was used to determine the periodicity of each submodel (Legendre, comm. pers.). RDAs were used to test the significance of each sub-model on the biological matrix. The significant axes were fitted in a model using a linear regression or RDA to identify the significant contribution of environmental variables in each sub-model. All multivariate analyses were conducted using the vegan 2.0-5 and PCNM package in the R language (Oksanen et al., 2012; R Core Development Team, 2008).

3. Results

3.1. Physical environment

While storms are common during winter in the northeast Subarctic Pacific, December 2011 was a relatively calm month in comparison to

November 2011 and January 2012 (Fig. 2; Juniper et al., in press). In November, the meteorological buoy near La Prouve Bank recorded strong winds reaching 0.6 N.m^{-2} , and surface wave heights reached 10 m at the end of the month (Fig. 2A). Water column currents in the range of the upward looking 150 kHz ADCP increased following these storms. This heightened current intensity penetrated to varying depths and tapered off towards the bottom. The strongest event began around November 26th and penetrated down to 840 m depth in the first days of December (Fig. 3). As an example, currents at 200 mab, which averaged 4 cm.s^{-1} during the entire period, reached 63 cm.s^{-1} on December 4th. In parallel, a shift in bottom water (890 m depth) physical properties began around November 27th. During the first 11 days of December, our study area was characterized by intrusions of colder and more saline water masses (Fig. 2B). Following this, temperature and salinity characteristics reverted to pre-December conditions. The de-tided bottom boundary layer currents, however, showed no significant heightened intensity over the same time period remaining well under 10 cm.s^{-1} with a persistent mean southerly flow of $\sim 5 \text{ cm.s}^{-1}$ (Fig. 2C). We could not therefore account for the change in water properties by a concomitant change in the local flow regime. In order to better understand the effects of tides and identify other significant oscillations in the very noisy raw current data we performed wavelet analysis of the dominant North-south component of the near bottom currents which were aligned with the local direction of the canyon (i.e. along isobaths). The analysis revealed local energy maxima at both the semi-diurnal and diurnal frequency bands, no apparent energy at the local near-inertial period of $\sim 16 \text{ h}$ and a broad feature at the 10–11 day period (Fig. 4). The tidal signals were not reminiscent of the deterministic nature of the barotropic tide but had the intermittency associated with an internal tide that was not phase-locked to the barotropic tide. The 10–11 day oscillation seemed to persist over the middle of the study period. Analysis of a year-long segment of these bottom currents indicates the oscillation to be an intermittent, but persistent feature of the region.

3.2. Fauna

A total of 6625 individuals belonging to 29 morphotypes and 6 phyla were observed over the entire period in the camera field of view (Fig. 5). The four dominant species were the shrimp *Heptacarpus* sp., the gastropod *B. viridum*, the sablefish *A. fimbria*, and the squat lobster *M. quadrata* (Table 2, Fig. 6). Except for the dominant species, densities were globally low with often only 1 individual of a species observed at a time (Table 2). A shift in dominant species from the shrimp *Heptacarpus* sp. to the gastropod *B. viridum* occurred approximately around December 11th (Fig. 6). Shrimp daily average abundance dropped from $5.8 (\pm 3.0)$ individuals per video during the first period, i.e. from December 1th to 11th, to $3.5 (\pm 2.2)$ individuals from December 12th to 31st. Buccinidae gastropods' abundances did not exceed 2 (1.4 ± 1.4) individuals at the beginning from December 1 to 11, while up to 14 individuals (4.7 ± 2.6) occurred in a single video on December 14th (see Table 2). For both species, densities were significantly different between both periods (Mann–Whitney U test, $p < 0.001$).

3.2.1. Biological rhythms

Periodogram analysis for the most abundant species (see Fig. 6), showed a composite scenario in behavioral rhythm regulation (Table 3). While no periodic signals were detected when analyzing the full month time-series, most dominant species showed weak rhythms depending on the 10-day time-series fragments considered (i.e. around 20% of variance, Table 3). Some species were consistently arrhythmic (i.e. *B. viridum* and *Eptatretus* sp.). Others showed a diel like rhythmicity with transient signs of internal tidal influences. *A. fimbria* exhibited weak 24-h periodicity from December 1 to 21, and a submultiple periodicity of 12-h from December 11 to 21. Such phenomena also seemed

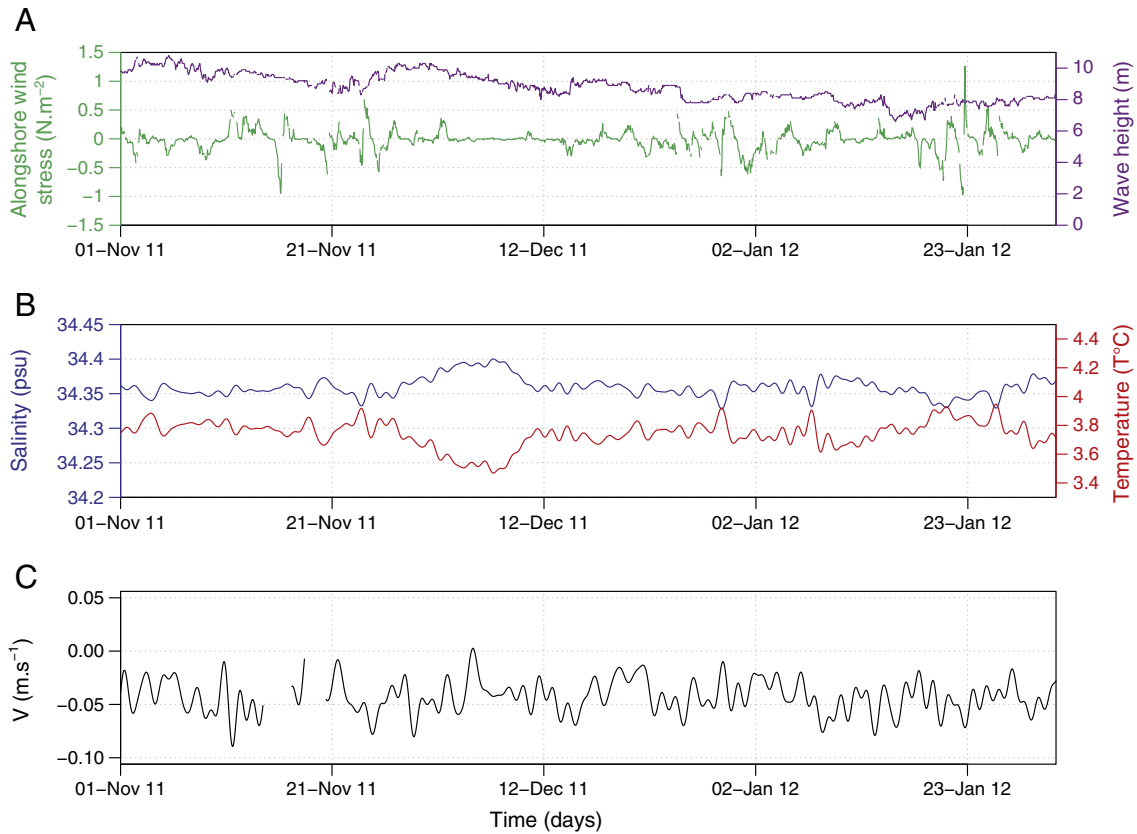


Fig. 2. Time-series of wind stress and wave heights (A), salinity and temperature (B), and along-axis bottom currents (C) from November 2011 to January 2012 in Barkley Canyon. Wind and wave data come from La Perouse Bank meteorological buoy, while current and water properties come from pods 3 and 4 instruments platform at 890 m depth in Barkley Canyon. Data are filtered to remove the tidal effects.

to be present in *M. quadrata*, although the submultiple periodicity (i.e. 15-h) correlated better with the inertial current frequency than the internal tides at the latitude of the study area (Table 3). In the case of the

pelagic shrimp, periodicity in activity rhythms was detected between December 1 and 10 but with less ecologically meaningful periodicities (Table 3). While no periodicity was detected between December 11

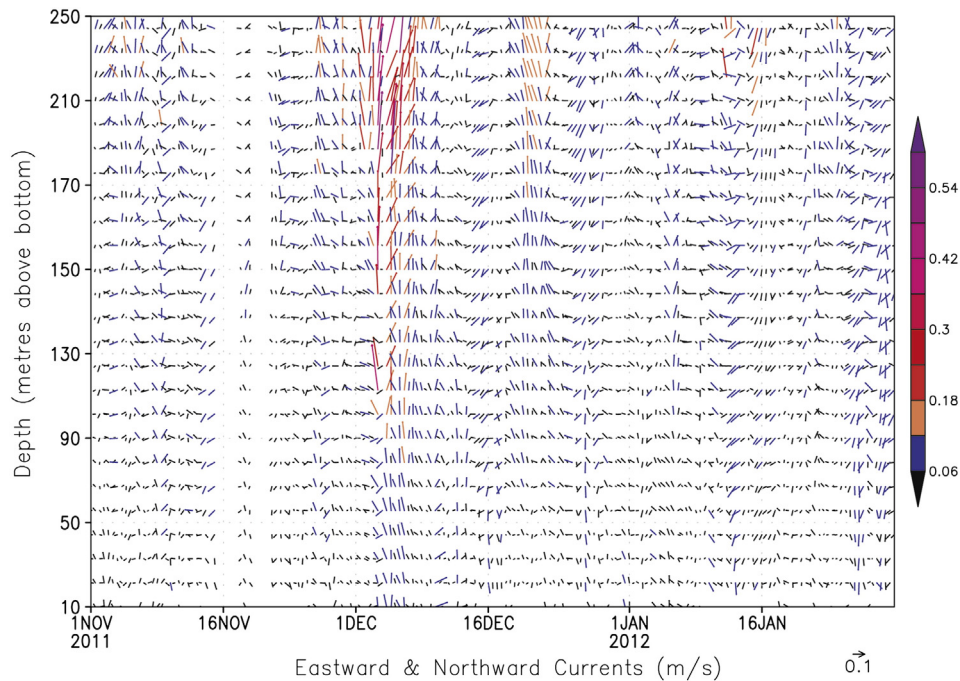


Fig. 3. Current profile in the water column between November 1st 2011 and January 31st 2012 in Barkley Canyon at the Pod 4 instrument platform. Data were acquired with a 150 kHz ADCP.

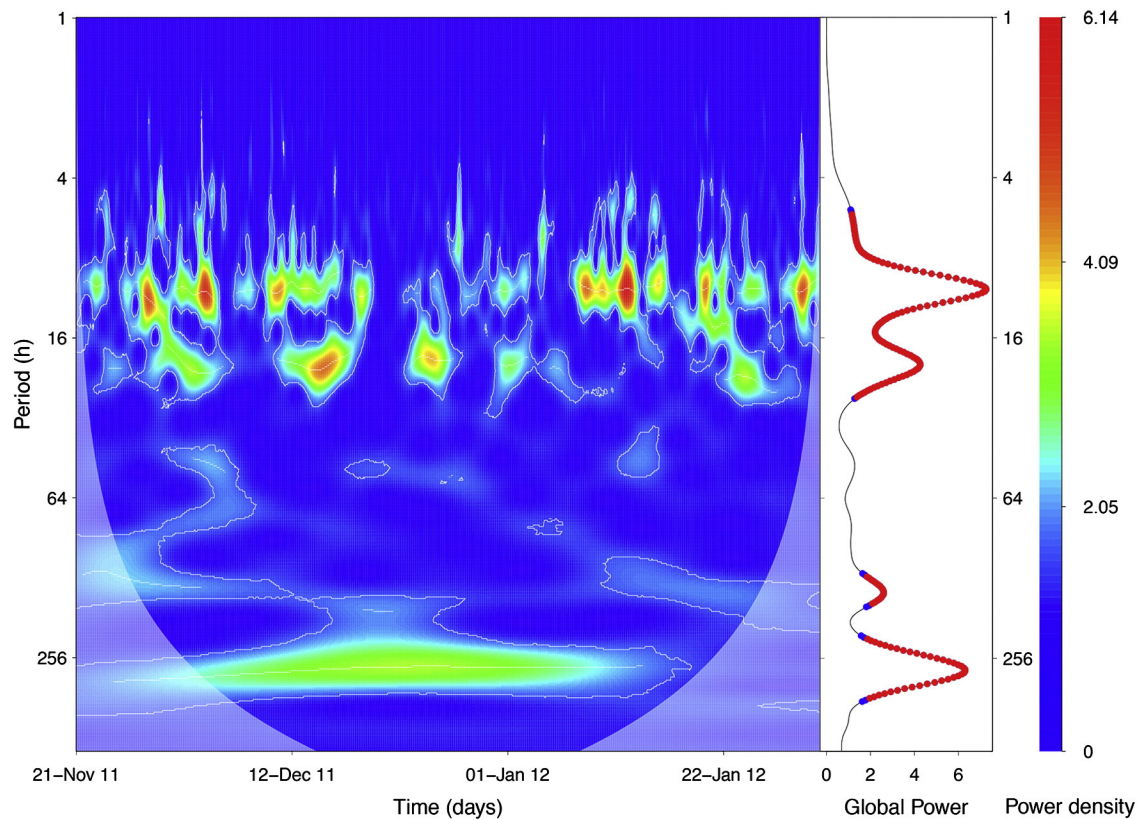


Fig. 4. Wavelet transform of bottom along axis current at 890 m depth in Barkley Canyon.

and 21, an internal tidal related rhythm was observable between December 22 and 31 with both a major and a submultiple periodicity (i.e. 24 and 11.4-h, respectively).

The waveform analyses described the results of Table 3 in terms of modifications in the diel (i.e. 24-h based) average visual count fluctuation within the selected three temporal intervals of video recording (Fig. 7). *A. fimbria* exhibited a temporal shift in the phase (i.e. values above the MESOR) moving from the second half of the day (i.e. December 1 to 10, 12:00–18:00 Pacific Standard Time-PST) to the first half of the night (i.e. December 11 to 20, 16:00–23:00 PST; December 22 to 31, 18:00 to 2:00 PST). In all cases, rhythm phase was not coincident with the phase of the water mass density or temperature fluctuations.

In the case of the squat lobster *M. quadrata* phase modifications over the three consecutive 10-day data sets were less evident. A weak

day-time phase occurred during the 2 first periods (i.e. December 1 to 10, 12:00–14:00 PST and December 11 to 21, 10:00–14:00 PST). This fluctuation was not present in the third segment of video recording (i.e. December 22 to 31). Instead, a periodicity of approximately 15 h was observed (see Table 3). At that time the phase was nocturnal (i.e. 16:00–22:00 PST) and coincided with peaks in water temperature and lows in water mass density.

With regard to the pelagic shrimp, a markedly different nocturnal phase was reported in almost all data segments (i.e. from approximately 22:00/00:00 to 4:00 PST), but another phase identification was difficult in the second waveform (i.e. December 11 to 21), yielding the arrhythmia detected in the periodogram analysis (see Table 3). In contrast with *M. quadrata*, the pelagic shrimp phase was more coincident with water density than with temperature.

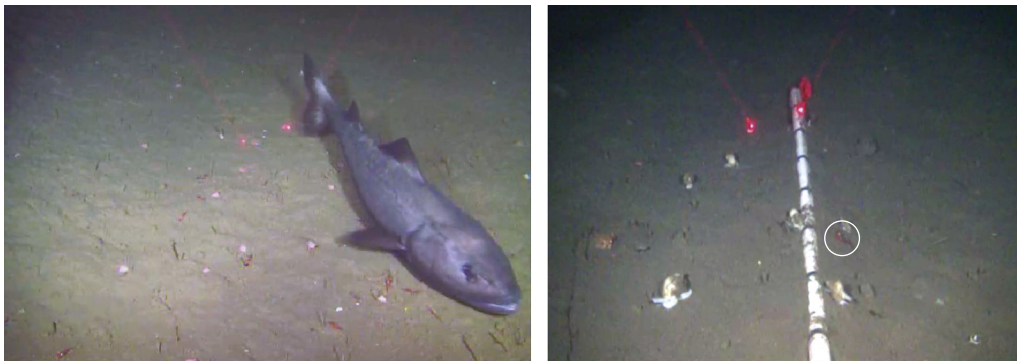


Fig. 5. Example of frames from the POD4 camera in Barkley Canyon at 890 m depth showing the scaling ruler on the seafloor. The two red laser points are separated by 10 cm. Left: the sablefish *Anoplopoma fimbria*. Right: the buccinid gastropod *Buccinum viridum* and the hippolytid *Heptacarpus* sp. (circled in white). (For interpretation of the references to color in this figure legend, the reader is referred to the web version of this article.)

Table 2
Daily average abundances of species encountered in the field of view of the camera in Barkley Canyon. Individuals were identified to the lowest taxonomic level possible. Total number corresponds to the total number of individuals counted per species over the entire period.

Day of December	1	2	3	4	5	6	7	8	9	10	11	12	13	14	15	16	17	18	19	20	21	22	23	24	25	26	27	28	29	30	31	Total nb.
<i>Chordates</i>																																
<i>Anoplopoma fimbria</i>	2	2.2	1.8	1.5	2.8	2.3	1.8	2.1	2.9	3.8	2	1.8	3	1.6	2.1	3.2	2.1	5.4	1.4	2.8	2.7	3.3	4.3	3.6	1.8	2.3	4.7	2.3	4.4	4.5	3.9	1033
<i>Eptatretus</i> sp.	0.5	0.3	0	0.1	0.9	0.4	0.2	0.2	0.4	0.3	0.3	0.6	0.3	0.2	0.6	0.4	0.8	0.7	0	0.3	1	0.3	0.5	0	0.3	0.4	1	0.4	0.3	0.5	0	145
Agonidae	0.3	0	0	0.2	0	0.1	0.3	0	0	0	0	0	0	0	0	0	0	0	0	0	0	0	0	0	0	0	0	0	0	0	0.5	16
Zoarcidae	0.2	0	0	0.1	0	0	0.2	0	0	0	0.2	0	0.1	0.4	0	0.1	0.2	0	0.7	1.1	0.3	0.4	0.2	0.1	0.3	0.1	0.3	0.3	0.2	0	0.1	63
<i>Coryphaenoides</i> sp.	0.1	0	0	0	0	0	0	0	0	0	0	0	0	0.1	0	0	0	0	0	0	0	0	0	0	0	0	0	0	0	0	0	2
<i>Sebastolobus</i> sp. 1	0.4	0.8	0.2	0.7	0.7	0.7	0.6	0.8	0.9	0.3	0.5	0.7	0.1	0	0.2	0.3	0.2	0	0.2	0.8	1.1	1.3	0.8	0.6	0.4	0.8	0.1	0.2	0.2	0.5	0	175
<i>Sebastolobus</i> sp. 2	0	0	0	0	0	0	0.1	0	0	0	0	0	0	0	0	0	0	0	0	0	0	0	0	0	0	0	0	0	0	0	0	1
<i>Arthropods</i>																																
<i>Chionoecetes tanneri</i>	0	0	0	0.1	0	0	0	0	0	0.1	0	0	0.2	0.1	0	0.1	0.1	0	0.3	0.1	0	0.3	0.3	0.3	0	0	0	0.6	0.4	0.6	1.4	59
<i>Paralomis verrilli</i>	0	0.2	0.1	0	0	0	0	0	0	0	0	0	0	0	0	0	0	0	0	0	0	0	0	0	0	0	0	0	0	0	0	3
Brachyura u. i.	0	0.1	0.1	0	0.1	0.2	1	0.3	0.1	0.1	0.3	0.1	0.3	0	0.8	0	0	0.3	1.3	0.3	0.1	0.1	0.3	0.1	0.6	0.9	0.3	0.8	0.8	0.8	1.8	138
Galatheaidea 1	0	0	0.1	0.4	0.2	0	0	0	0	0	0.2	0.1	0.3	0.1	0	0.1	0	0	0.2	0.1	0	0	0	0	0	0.1	0.2	0.1	0	0.3	0	27
<i>Munidopsis quadrata</i>	1.4	1.9	1.8	1.7	1.8	0.8	2.1	2.3	1.7	1.6	1.8	2.4	2.3	2	2.4	2.8	3	1.6	2.3	3	2	2.7	0.7	1.8	2.2	2.6	2.8	3	2.9	1.4	0.8	759
<i>Heptacarpus</i> sp.	4.7	5.3	6.1	8.4	5.3	6.3	5.4	5.8	5.9	5.1	5.5	4.6	3.7	2.6	5	5.5	5.1	2.1	3.5	5.2	2.5	2.8	1.5	2.2	1.5	2.5	2.8	4.3	3.7	3.4	4.8	1597
Caridea (pelagic)	0.8	0.8	0.6	0.1	0.5	1.2	0.8	0.3	0.6	0.3	0.5	0.5	1.1	0.5	1.6	1.5	0.5	0.7	0.5	0.8	0.8	1.3	0.8	0.6	0.3	0.3	1	0.9	1.5	0.6	0.7	274
Pandaloidea	0	0	0	0.7	0.3	0.3	0.1	0	0	0	0	0	0	0	0	0	0	0	0.1	0.5	0.5	0.2	0	0	0	0	0	0	0	0	0	31
Paguroidea	0	0.3	0.1	0.2	0.3	0	0	0	0	0.6	0.2	0	0	0	0.2	0.2	0.2	0	0.5	0.1	0.2	0.7	0	0	0	0	0	0	0	0	0	42
<i>Molluscs</i>																																
<i>Buccinum viridum</i>	1.9	1.3	0.4	1.1	1.5	1	1.2	0.3	1.3	2.2	3.2	2.3	2.6	11	5.4	6.4	6.7	2.8	2.7	3.3	5.3	4.1	6.3	3.8	3.2	5.8	4.4	5.3	4	3.7	4.8	1300
Gastropoda 1	0	0	0.2	0.9	0.1	0	0.3	0.3	0	0	0.1	0	1.1	1	0.1	0.3	0.1	0	0.3	0.3	0	0.8	0.4	0.2	0.9	0	0	0	0	1	99	
Cirripedia	0	0	0	0	0	0	0	0	0	0	0	0	0	0	0	0	0	0	0	0	0	0.3	0.1	0	0	0	0	0	0	0.2	7	
<i>Echinoderms</i>																																
Asteriidae	0	0	0	0	0	0	0	0	0	0	0	0	0	0	0	0	0	0.8	0.8	0	0	0	0	0	0.9	0.8	0	0	0	0.7	1	61
Hippasterinae	0	0	0	0	0	0	0	0	0	0	0	0	0	0	0	0	0	0	0	0	0	0.1	0	0	0	0	0	0	0	0	0	1
<i>Panmychiamoseleyi</i>	0.1	1	1	1	1.3	1	1	1	1	1	1	1	1.3	1.9	2	2	2	1.9	0.9	0.8	0	0	0	0	0.2	0.3	0	0	0	0	0	294
<i>Cnidarians</i>																																
<i>Poralia rufescens</i>	0	0.1	0	0	0	0	0	0	0.2	0.1	0	0	0.1	0.1	0	0.1	0	0	0.1	0	0	0	0	0	0.1	0	0	0.1	0	0	0	10
Scyphozoa	0	0	0.1	0	0.1	0	0.1	0	0	0	0	0	0	0	0	0	0	0	0	0.1	0	0	0	0	0	0	0	0.1	0.1	0.1	0	7
Ctenophores	0	0	0	0	0	0	0	0	0	0	0	0	0	0	0	0	0	0	0	0	0	0	0	0.2	0	0.1	0	0	0	0	0	3

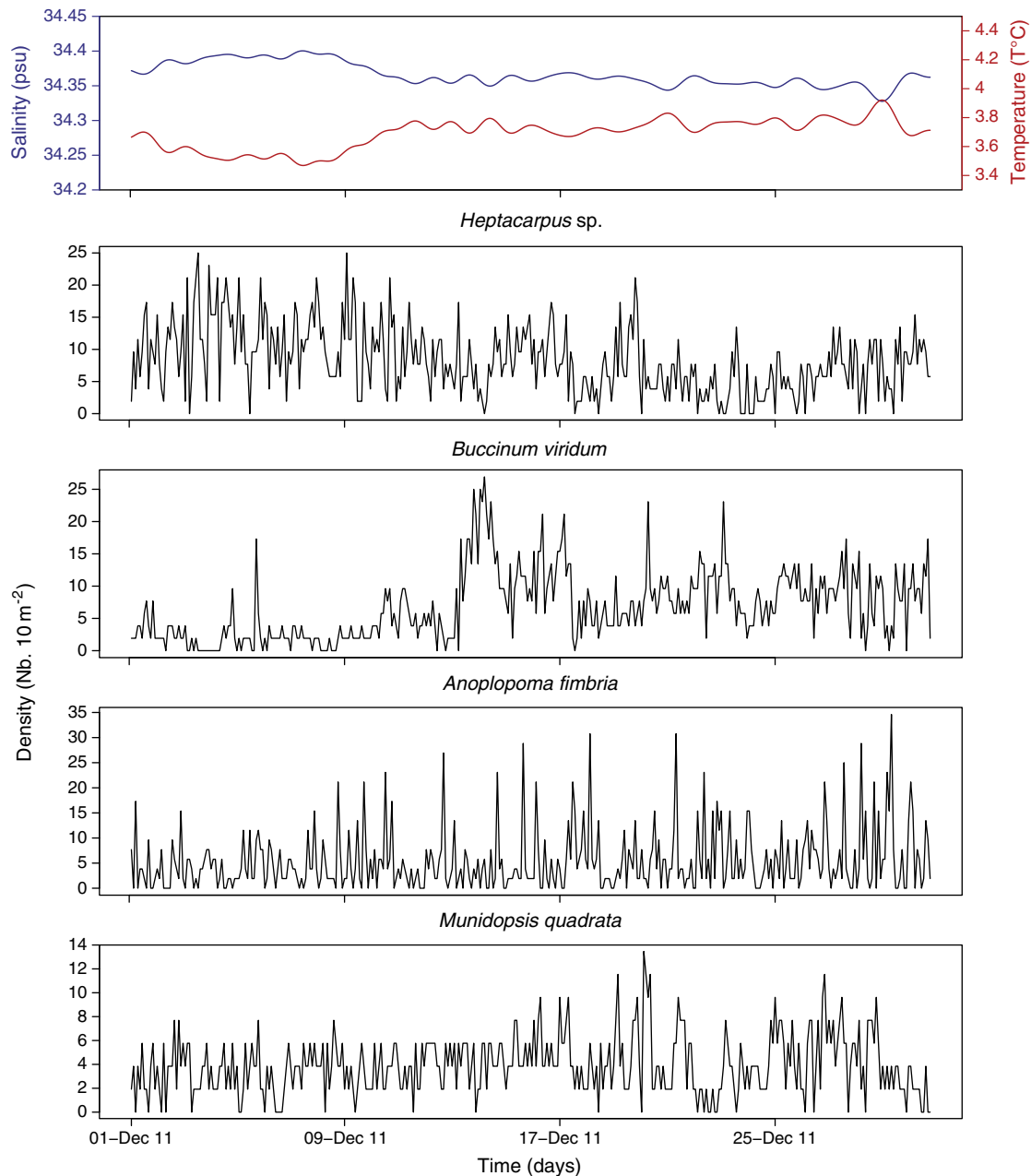


Fig. 6. Densities of the 4 dominant species observed in the camera field of view at the Barkley Canyon site. Note the difference of scale among species.

3.2.2. Community dynamics and influence of the environment

The set of environmental variables considered in this study accounted for 17.3% of the total variance in the density data. The first axis of the redundancy analysis biplot explained 10.9% of the total variance and separated observations made at the beginning and the end of the month with a transition around December 11–15 (Fig. 8). The RDA highlighted two states in the epibenthic community structure: one dominated by the shrimp *Heptacarpus sp.*, associated with cold salty water occurring at the beginning of the month, and the other where the buccinids dominated in a warmer, less salty water. Along the second axis, which explained 6.1% of the total variance, sablefish (*A. fimbria*) density was highly correlated with resuspension events and inversely correlated with visibility, as expected from visual observations. A linear trend explaining 10.2% of the total variance observed was detected and was significantly related to water properties (i.e. salinity, temperature, density). After detrending, the environmental data

only explained 8.7% of the total variance and only temperature, visibility and resuspension events remained significant variables (Table 4).

The dbMEM analysis, performed on the detrended density data, revealed the temporal structure of the benthic community observed in the field of view of the camera over the month. Four scales were defined: broad (10–12 days), medium (5–6 days), fine (2–3 days) and very fine (12–24 h) scales. The broad scale accounted for 7.1% of the total variance in the species density data and was significantly correlated to water mass properties (i.e. temperature, salinity and density, and bottom currents magnitude) (Table 4). This shift in environmental conditions was visible in the physical data around December 11th (Figs. 2 and 3). The medium and fine scales explained 4.2% and 8.5% of the total variance, respectively, and were not correlated with any of the tested environmental variables in this study. Finally, the very fine scale (i.e. 6.4% of the variance) was significantly correlated with visibility (Table 4) which is probably related with the diurnal rhythmic

Table 3

Significant periodicities (P; 24-h based) and submultiples (S; internal tide-based) detected by periodogram analysis in visual counts time-series of 10-day duration, as obtained from the inspection of temporally scheduled filming in Barkley Canyon. The % of variance of peaks in periodogram output plots is also reported as a marker of rhythms strength. Arrhythmia (arr.) as well as the absence of significant periodicities as submultiples of P (–) are also reported.

	Time-series fragments (10-days)											
	1–10				11–21				22–31			
	P	%	S	%	P	%	S	%	P	%	S	%
<i>A. fimbria</i>	23.4	22.7	–	–	24.3	17.7	12.2	10.7	arr.			
<i>B. viridum</i>	arr.				arr.				arr.			
<i>Eptatretus</i> sp.	arr.				arr.				arr.			
<i>Heptacarpus</i> sp.	26.3	23.8	13	11.6	arr.				arr.			
<i>M. quadrata</i>	24.1	17.2	–	–	24	19.3	15.4	15	–	–	15.1	11.3
Caridea (pelagic)	26.2	24.3	13	11.3	arr.				24.5	17.6	11.4	10.4

activity of *A. fimbria* (see Table 3) which causes resuspension events by abrupt displacement (pers. obs.).

4. Discussion

In this multidisciplinary study we were able to quantitatively relate temporal abundance changes of species to concomitant variations in the properties and dynamics of the surrounding water mass at fine temporal scales. This demonstration of the potential of cabled observatories represents an important beginning for the understanding of the dynamics of deep-sea communities (Glover et al., 2010; Levin and Sibuet, 2012). These kinds of studies are essential since they can directly link community-level patterns to the behavior of single individuals (Aguzzi et al., 2012a).

This approach has some limitations. The presence of the observatory platform and the use of intense white light can affect species behavior, particularly in deep-sea fishes (Widder et al., 2005). In the literature, the influence of light on the sablefish *A. fimbria* is unclear: while a study from an ROV showed little impact of white light on this species (Krieger, 1997), Widder et al. (2005) documented an increase in *A. fimbria* abundance under red light compared to white light and suggested that the species avoids white light by escaping. In a recent study at our Barkley Canyon site, sablefish individuals are first attracted by the lights and then exit the field of view after a certain time of illumination (Doya et al., 2013). White light did not seem to affect the hagfish *Eptetratus* sp. which has reduced eyes with no lenses (Widder et al., 2005). Other species of fish were rare in this study and nothing is known about their behavioral response to light. There is little information on the influence of light on invertebrates, but considering their low swimming ability, a short duration of light is unlikely to affect their presence/absence in the field of view. Another source of disturbance includes electrical noises, vibrations and increased temperature. However, a study of the effect of instrument platform structures conducted in the North East Pacific showed no influences on megafaunal abundance (Vardaro et al., 2007). In addition, the lighting (60 min per day) and seafloor platform structure were constant throughout the study and we are therefore confident that the observed changes were linked to external factors as previously suggested (Matabos et al., 2012).

4.1. Physical environment

Values of wind stress and wave height recorded at the surface in November and beginning of December in our study area were characteristics of the trajectory of low pressure systems and the beginning of local storm season. During the summer months a semi-permanent high tends to deflect these storm tracks to the north (Thomson, 1981). As a result of this intensification of atmospheric forcing, instruments deployed on the seafloor at 890 m depth revealed an increase in water current speed in the deep-water column 10 days following the first strong surface winds. Although oscillations at the inertial frequency

were not evident in the bottom boundary layer, strong storms can generate inertial wave propagation deeper than 800 m depth and have been suggested to play an important role in deep-water mixing processes (Alford et al., 2012). From our observations the shift in water mass properties observed at 890 m depth following the storm cannot be attributable to the direct mixing effect of downward propagating wind-forced inertial waves; it is more likely due to remote mixing by the storm generated currents being advected into the region by the persistent southerly currents. The arrival of these slightly denser waters in December 2011 was one of the major events recorded over that year at that depth in Barkley Canyon (Juniper et al., in press). Surface wind-induced upwelling is common on the west coast of North America, and is more common during summer when northerly winds dominate in the area (Freeland and Denman, 1982). However, in a one-year study Juniper et al. (in press) saw no signature of seasonal upwelling in 2011 at 900 m depth, while a shallower site on the NEPTUNE Canada network (i.e. 100 m depth) revealed strong upwelling during summer months. This implies that wind-induced Ekman transport at the surface over the shelf does not drive upwelling at these depths on the continental slope. As an alternative mechanism, the runoff and resuspension created by the storms can also contribute to an abrupt shift in hydrographic properties by inducing downslope turbidity currents in this steeply sloped region. Again, although not directly observed at the location of our measurements, the downward propagation of these flows will displace deeper cooler saltier water to higher elevations which can be advected into the study areas (see Simpson, 1982). More investigations are needed to understand the origin and causes of such events.

4.2. Biological rhythms and temporal community structure

The species encountered in this study can be classified into three main groups according to their locomotory capability (Aguzzi et al., 2010): ‘crawlers’ (i.e. echinoderms and molluscs) with limited mobility, and more active ‘walkers’ and ‘swimmers’ (i.e. crustaceans and fishes). The only abundant crawler was *B. viridum* species, which did not show any rhythmic activity at the daily scale. For almost all other dominant species, we detected diel variations in visual counts only when dividing the full time-series into 10-day segments. A higher sampling frequency (i.e. at least hourly observations) could provide higher abundances, thus reducing variation in the data, resulting in more power to detect activity rhythms over the month. For example, the shrimp *Heptacarpus* sp. displayed a rhythmic behavior only during the first period when abundance reached 25 individuals per 10 m². However, even a study (Doya et al., 2013) based on a 30-minute sampling frequency with the same camera only revealed significant diel rhythmic visual count fluctuations for the sablefish *A. fimbria*. Doya et al. suggested that abundances of the other invertebrates were too variable to reveal any discernible patterns of temporal variation. For rhythmic species, density phases were coincident with water temperature or water density, which were inversely correlated. This suggested that the diel

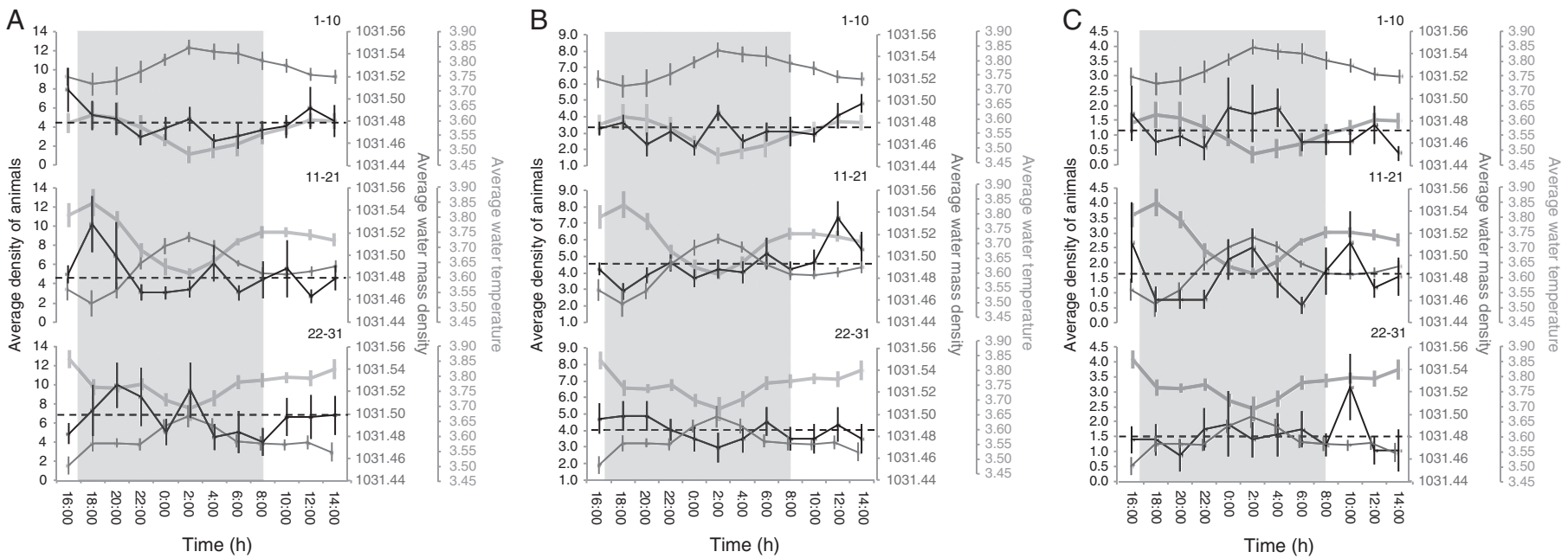


Fig. 7. Waveform analysis outputs of time-series in visual counts (black) for the sablefish *Anoplopoma fimbria* (A), the squat lobster *Munidopsis quadrata* (B), and the pelagic shrimp (C), and concomitant habitat variation (i.e. water density, dark gray; water temperature, light-thick gray) as reported by temporally scheduled video recording of the NEPTUNE camera at Barkley mid-canyon. Dashed horizontal line is the MESOR for average visual counts sets. The shaded area represents the night time. Time is in Pacific Standard Time-PST.

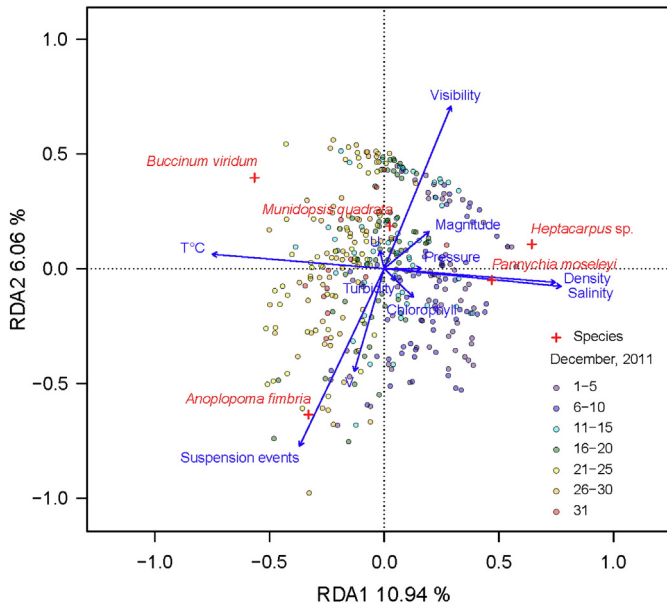


Fig. 8. Redundancy analysis correlation biplot of the observations, species (red) and environmental variables (blue) in Barkley Canyon. The redundancy analysis is based on the non-detrended species density data. T°C: Temperature in °C, U: East-west cross-axis current speed, and V: North-south along-axis current speed (m.s⁻¹). (For interpretation of the references to color in this figure legend, the reader is referred to the web version of this article.).

variations detected in the 4 species were related to tidal oscillations, which have been reported as the main driver for rhythmic behavior in the deep sea (Aguzzi et al., 2010). Animals may vary their rate of behavioral activity as current speed increases in order to reduce movement drag and maintain their geographic location. In Saanich Inlet, a coastal fjord on Southern Vancouver Island, a closely related species to the hippolytid shrimp *Heptacarpus* sp., *Spirontocaris sica*, also exhibited a weak tidal signal (Matabos et al., 2011).

A shift in the dominant species occurred around December 10th from *Heptacarpus* sp. to *B. viridum*. This shift was coincident with the observed change in water masses in terms of density, temperature

Table 4

R² and probabilities related to the temporal analysis of the detrended species density data at Barkley Canyon. First line: R² of each temporal submodel. Second line: R² of the regression of the submodel (fitted values) on environmental variables. Third line: product of the two previous lines, i.e. variation of the species density data explained by the environmental variables at the scale considered. Other lines: p-values of the regression coefficients of the environmental variables in the model considered. * are significant p-values.

	All	Broad 10–12 days	Medium 5–6 days	Fine 2–3 days	Very fine 12–24 h
R ² submodel on community	–	0.071	0.042	0.085	0.064
R ² environment on submodel	–	0.113*	–0.002	0.007	0.021*
R ² environment on community	0.087	0.008	0.000	0.001	0.001
Density	0.080	0.001*	0.397	0.728	0.603
T°C	0.043*	0.001*	0.330	0.624	0.409
Salinity	0.088	0.002*	0.442	0.713	0.718
Pressure	0.085	0.001*	0.430	0.726	0.627
Turbidity	0.380	0.102	0.102	0.754	0.462
Chlorophyll	0.880	0.152	0.984	0.746	0.516
U	0.850	0.382	0.850	0.897	0.345
V	0.005*	0.100	0.442	0.217	0.884
Magnitude	0.054	0.045*	0.696	0.137	0.463
Visibility	0.005*	0.601	0.990	0.983	0.033*
Suspension event	0.005*	0.992	0.287	0.629	0.107

and salinity, as well as current magnitude in the water column (Figs. 3 and 6).

The gradual disappearance of the shrimp *Heptacarpus* sp. starting on December 10th was difficult to explain. The closely related species *S. sica* in Saanich Inlet inhabits the oxygen fluctuation zone of the fjord where low dissolved oxygen concentrations are balanced by factors such as increased food availability (i.e. bacterial mats) and reduced predation pressure (Matabos et al., 2012). Individuals perform a nekto-benthic migration along the slope to follow the minimum oxygen zone that varies from year to year depending on oxygen depletion and deep-water renewal events. However, potential dissolved oxygen concentration variations over the year at this site were likely too weak to have caused shrimp population migration. The depth of the study site corresponds to the core of the oxygen minimum zone in the North Pacific, where oxygen concentrations are less than 0.5 ml.l⁻¹ as measured by the CTD-O₂ profilers at nearby Ocean Station P4 (<http://www.pac.dfo-mpo.gc.ca/science/oceans/data-donnees/line-p/index-eng.htm>). In addition, the Barkley Canyon mid-slope study site is below the zone where O₂ concentrations would be expected to be influenced by upwelling (Juniper et al., press). On the other hand, the observation of the shrimp populations at the seafloor coincided with enhanced, storm-related currents in the water column. Because of its relatively small size, this shrimp is likely a weak swimmer under the influence of hydrodynamic conditions, and our results suggest that animals could have migrated to the deeper zones to avoid stronger currents. On the Canadian Atlantic coast, the lobster *Homarus americanus* performs a seasonal mass migration where individuals move to deeper water in autumn in response to increase turbulence due to storms (Ennis, 1983). The shrimp could avoid strong currents by moving downslope and then returning when conditions become milder, such as in the middle of December. A combination of longer time-series with a multi-disciplinary approach will allow comparisons between calm and storm periods to confirm this hypothesis.

The gastropod *B. viridum* exhibited the opposite trend in comparison to the shrimp with increasing densities after December 12th. Buccinids are strictly benthic, so likely not affected by currents in the first 200 m of the water column above the bottom. They are predators and scavengers, known to form aggregations to exploit prey (Lapointe and Sainte-Marie, 1992), to mate (Himmelman and Hamel, 1993) and to avoid unfavorable conditions (Theede, 1973). No predation or intra- or inter-species interactions were documented in this study, and there is no information available regarding their reproduction. The arrival of individuals about 4–5 cm in size does not support the occurrence of a recruitment event but rather is likely the result of a population migration. On the other hand, if *B. viridum* also migrated from shallower waters or from the axis of the canyon to avoid enhanced currents, their limited displacement ability would explain the delay of arrival in the study area compared with the swimming shrimp *Heptacarpus* sp. However, the camera's limited areal coverage does not allow the determination of whether or not this increase in density corresponded to aggregation behavior or population movement, or at what spatial scale any aggregations occurred. Buccinid behavioral ecology is poorly understood in the deep sea but they may exploit changes in current speed and direction in order to locate (odor sensing) sparse food sources, often carrion, which can be quickly consumed following the arrival of scavengers (Aguzzi et al., 2012b).

4.3. Environmental drivers: a matter of scales

In the deep sea, inertial and internal tidal currents create temporal and geographically highly variable hydrodynamic patterns, and it is now recognized that these oscillations influence activity rhythms of deep-sea species (Aguzzi et al., 2011). Our results showed that depending on the time period considered and the sampling frequency, such rhythms are more or less evident. Here, the subdivision of the time-series into three 10-day segments revealed the variable occurrence

of activity rhythm within a single species. Organism responses to environmental events can be stronger than biological rhythm signals and can compromise their detection. For example, in most decapods, day-night or tidal based activity can be masked by competition for substrata (Aguzzi et al., 2009), food availability (Fernández de Miguel and Aréchiga, 1994) and dissolved oxygen fluctuations (Matabos et al., 2011; Schurmann et al., 1998). Here, the shift in community structure related to changes in water mass properties and bottom currents acting over a longer temporal scale (i.e. 11 days) might explain the variability in activity rhythms detected over the month. The surface storm probably generated enhanced bottom currents via the canyon, possibly affecting sediment transport (Sanchez-Vidal et al., 2012), and thus food availability and habitat for the benthic community. While it is impossible to directly link surface storms to the observed variations in water mass characteristics (i.e. upwelling of slight denser water/cascading), changes in bottom currents and/or water properties coincided with, directly or indirectly, population movements for at least two species. Our results support the growing idea that surface storms can influence deep sea ecosystems (Alford et al., 2012; Sanchez-Vidal et al., 2012). Large fish with strong swimming abilities (i.e. *A. fimbria* and *Eptetratus* sp.) did not seem to be affected by these water property changes. The distance-based Moran's Eigenvectors Map also revealed a structure on the scale of 5–6 days and 2–3 days respectively; however none of the environmental variables considered in this study explained these patterns, which we propose could be related to biotic factors like predation or competition, or species life-history traits.

It will be essential to maintain the time-series to confirm the patterns and hypothesis highlighted in this study, as well as to conduct parallel sampling and video transects to integrate the results in a spatial dimension. Indeed, at this stage it would be premature to extrapolate observations at such a small scale to the entire area, and the study needs to be extended to other sites in order to increase our understanding of this system. We recommend conducting video transects during NC maintenance cruises in order to provide broader scale information on species distribution and habitat heterogeneity at different times of the year. The use of cameras at different depths will also give insight on population movements following changes in environmental conditions. Understanding decadal and longer-term trends in species abundance and distribution represents an important challenge for future research on continental margins, where climate change combined with increasing human activities place pressures on marine biodiversity and ecosystem functioning (Levin and Sibuet, 2012). Until natural higher frequency variability is better understood, it will be difficult to interpret any long-term trends that may be apparent in data sets. As well, understanding cause and effect relationships between environmental variables and faunal responses will require experimental manipulation and multi-disciplinary observatory studies (Aguzzi et al., 2012a). The causes of the water mass changes observed in this study were not fully explained by the current data, and longer, high-frequency time-series are needed to provide the resolution necessary to understand the underlying processes. This study constitutes a first step towards fine-scale characterization of deep benthic communities and provides knowledge of species behavior and activity. We are convinced that these types of multidisciplinary studies are needed for future experiments in Barkley Canyon in order to understand factors acting at larger temporal scale. NEPTUNE Canada data are freely available through the Oceans 2.0 software (<http://dmas.ubic.ca>).

Acknowledgments

Funding for the Barkley Canyon instruments and installation was provided by the Canada Foundation for Innovation and the British Columbia Knowledge Development Fund. Funding for time-series analyses was given by the RITFIM project (PI: J. Aguzzi; CTM2010-16274; Ministerio de Ciencia e Innovación-MICINN). We thank Françoise Gervais and Alex Spicer for their help in species identification, and

Damian Grundle for his valuable comments on a previous version of the manuscript. We thank the ROPOS ROV team and the crews of the CCGS John P. Tully and R/V Thomas G. Thompson for their assistance in the field. J. Aguzzi is a Postdoctoral Fellow of the Ramón y Cajal Program (MICINN).

References

- Aguzzi, J., Company, J.B., 2010. Chronobiology of deep-water decapod crustaceans on continental margins. *Adv. Mar. Biol.* 58, 155–225.
- Aguzzi, J., Sarda, F., Abello, P., Company, J.B., Rotllant, G., 2003. Diel and seasonal patterns of *Nephrops norvegicus* (decapoda: Nephropidae) catchability in the western Mediterranean. *Mar. Ecol. Prog. Ser.* 258, 201–211.
- Aguzzi, J., Bahamon, N., Marotta, L., 2009. The influence of light availability and predatory behaviour of the decapod crustacean *Nephrops norvegicus* on the activity rhythms of continental margin prey decapods. *Mar. Ecol. Prog. Ser.* 306, 366–375.
- Aguzzi, J., Costa, C., Furushima, Y., Chiesa, J., Company, J., Menesatti, P., Iwase, R., Fujiwara, Y., 2010. Behavioral rhythms of hydrocarbon seep fauna in relation to internal tides. *Mar. Ecol. Prog. Ser.* 418, 47–56.
- Aguzzi, J., Company, J.B., Costa, C., Menesatti, P., Garcia, J.A., Bahamon, N., Puig, P., Sarda, F., 2011. Activity rhythms in the deep-sea: a chronobiological approach. *Front. Biosci.* 16, 131–150.
- Aguzzi, J., Company, J.B., Bahamon, N., Flexas, M.M., Tecchio, S., Fernandez-Arcaya, U., Garcia, J.A., Mechó, A., Koenig, S., Canals, M., 2012. Deep-sea buccinid gastropods scavenging behaviour under natural and simulated food-fall conditions. *Mar. Ecol. Prog. Ser.* 458, 247–253.
- Aguzzi, J., Company, J.B., Costa, C., Matabos, M., Azzurro, E., Manuel, A., Menesatti, P., Sarda, F., Canals, M., Delory, E., Cline, D.E., Favali, P., Juniper, S.K., Furushima, Y., Fujiwara, Y., Chiesa, J.J., Marotta, L., Bahamon, N., Priede, I.G., 2012. Challenges to the assessment of benthic populations and biodiversity as a result of rhythmic behaviour: video solutions from cabled observatories. *Oceanogr. Mar. Biol.* 50, 233–284.
- Alford, M.H., Cronin, M.F., Klymak, J.M., 2012. Annual cycle and depth penetration of wind-generated near-inertial internal waves at ocean station Papa in the northeast Pacific. *J. Phys. Oceanogr.* 42, 889–909.
- Angeles, D.G., Viedma, O., Moreno, J.M., 2009. Statistical performance and information content of time lag analysis and redundancy analysis in time series modeling. *Ecology* 90, 3245–3257.
- Arntz, W.E., Gallardo, V.A., Gutiérrez, D., Isla, E., Levin, L.A., Mendo, J., Neira, C., Rowe, G.T., Tarazona, J., Wolff, M., 2006. El Niño and similar perturbation effects on the benthos of the Humboldt, California, and Benguela Current upwelling ecosystems. *Adv. Geosci.* 1983, 243–265.
- Billett, D.S.M., Bett, B.J., Reid, W.D.K., Boorman, B., Priede, I.G., 2010. Long-term change in the abyssal NE Atlantic: the “Amperima Event” revisited. *Deep-Sea Res. II* 57, 1406–1417.
- Blanchard, A.L., Feder, H.M., Hoberg, M.K., 2010. Temporal variability of benthic communities in an Alaskan glacial fjord, 1971–2007. *Mar. Environ. Res.* 69, 95–107.
- Borcard, D., Legendre, P., 2002. All-scale spatial analysis of ecological data by means of principal coordinates of neighbour matrices. *Ecol. Model.* 153, 51–68.
- Carney, R.S., 2005. Zonation of deep biota on continental margins. *Oceanogr. Mar. Biol.* 43, 211–278.
- Chiesa, J.J., Aguzzi, J., García, J.A., Sardà, F., De La Iglesia, H.O., 2010. Light intensity determines temporal niche switching of behavioral activity in deep-water *Nephrops norvegicus* (Crustacea: Decapoda). *J. Biol. Rhythm.* 25, 277–287.
- Company, J.B., Ramirez-Llodra, E., Sarda, F., Puig, P., Canals, M., Calafat, A., Palanques, A., et al., 2011. Submarine canyons in the Catalan Sea (NW Mediterranean): megafaunal biodiversity patterns and anthropogenic threats. In: Wurz, M. (Ed.), *Mediterranean Submarine Canyons: Ecology and Governance*. Solprint, Gland (Switzerland) and Malaga (Spain), pp. 133–144.
- Doya, C., Aguzzi, J., Pardo, M., Matabos, M., Company, J.B., Costa, C., Mihaly, S., Canals, M., 2013. Diel behavioural rhythms in sablefish (*Anaplopoma fimbria*) and others benthic species, as recorded by the Deep-sea cabled observatories in Barkley Canyon (NEPTUNE-Canada). *J. Mar. Syst.* <http://dx.doi.org/10.1016/j.jmarsys.2013.04.003>.
- Emery, W.J., Thomson, R.E., 1997. *Data Analysis Methods in Physical Oceanography*. Pergamon Press, Exeter, UK (634 pp.).
- Ennis, G.P., 1983. Observations on the behavior and activity of lobsters, *Homarus americanus*, in nature. *Can. Tech. Rep. Fish. Aquat. Sci.* 1165 (St John's, New Foundland).
- Fernández de Miguel, F., Aréchiga, H., 1994. Circadian locomotor activity and its entrainment by food in the crayfish *Procambarus clarkii*. *J. Exp. Biol.* 190, 9–21.
- Freeland, H.J., Denman, K., 1982. A topographically controlled upwelling center off southern Vancouver Island. *J. Mar. Res.* 40, 1069–1093.
- Glover, A.G., Gooday, A.J., Bailey, D.M., Billett, D.S.M., Chevaldonné, P., Colaço, A., Copley, J., Cuvelier, D., Desbruyères, D., Kalogeropoulou, V., Klages, M., Lampadariou, N., Lejeune, C., Mestre, N.C., Paterson, G.L.J., Perez, T., Ruhl, H., Sarrazin, J., Soltwedel, T., Soto, E.H., Thatje, S., Tselepidis, A., Van Gaever, S., Vanreusel, A., 2010. Temporal change in deep-sea benthic ecosystems: a review of the evidence from recent time-series studies. *Adv. Mar. Biol.* 58, 1–95.
- Himmelman, J.H., Hamel, J.R., 1993. Diet, behaviour and reproduction of the whelk *Buccinum undatum* in the northern Gulf of St. Lawrence, eastern Canada. *Mar. Biol.* 116, 423–430.
- Juniper, S.K., Matabos, M., Mihaly, S., Ajayamohan, R.S., Gervais, F., 2013. A year in Barkley Canyon: a time-series observatory study of mid-slope benthos and habitat dynamics using the NEPTUNE Canada network. *Deep-Sea Res.* <http://dx.doi.org/10.1016/j.dsr2.2013.03.038i> II.

- Krieger, K.J., 1997. Sablefish, *Anoplopoma fimbria*, observed from a manned submersible. In: Saunders, M., Wilkens, M. (Eds.), *Biology and Management of Sablefish, Anoplopoma fimbria*: U.S. Dep. Commer., NOAA Tech. Rep. NMFS, 130, pp. 39–43.
- Lapointe, V., Sainte-Marie, B., 1992. Currents, predators, and the aggregation of the gastropod *Buccinum undatum* around bait. *Mar. Ecol. Prog. Ser.* 85, 245–257.
- Legendre, P., Legendre, L., 1998. *Numerical Ecology*, second. Elsevier, Amsterdam.
- Levin, L.A., Sibuet, M., 2012. Understanding continental margin biodiversity: a new imperative. *Ann. Rev. Mar. Sci.* 4, 79–112.
- Levin, L.A., Sibuet, M., Gooday, A.J., Smith, C.R., Vanreusel, A., 2010. The roles of habitat heterogeneity in generating and maintaining biodiversity on continental margins: an introduction. *Mar. Ecol.* 31, 1–5.
- Matabos, M., Aguzzi, J., Robert, K., Costa, C., Menesatti, P., Company, J.B., Juniper, S.K., 2011. Multi-parametric study of behavioural modulation in demersal decapods at the VENUS cabled observatory in Saanich Inlet, British Columbia, Canada. *J. Exp. Mar. Biol. Ecol.* 401, 89–96.
- Matabos, M., Tunnicliffe, V., Juniper, S.K., Dean, C., 2012. A year in hypoxia: epibenthic community responses to severe oxygen deficit at a subsea observatory in a coastal inlet. *PLoS One* 7.
- Menot, L., Sibuet, M., Carney, R.S., Levin, L.A., Rowe, G.T., Billett, D.S.M., Poore, G., Kitazato, H., Vanreusel, A., Galéron, J., Lavrado, H.P., Sellanes, J., Ingole, B.S., Krylova, E., 2010. New perceptions of continental margin biodiversity. In: McIntyre, A.D. (Ed.), *Life in World's Oceans: Diversity, Distribution, and Abundance*. Oxford, UK, Wiley Blackwell, pp. 79–102.
- Oksanen, J., Blanchet, F.G., Kindt, R., Legendre, P., Minchin, P.R., O'Hara, R.B., Simpson, G.L., Solymos, P., Stevens, M.H.H., Wagner, H., 2012. *Vegan: Community Ecology Package*. R package version 2.0-4. (<http://CRAN.R-project.org/package=vegan>).
- Papiol, V., Cartes, J.E., Fanelli, E., Maynou, F., 2012. Influence of environmental variables on the spatio-temporal dynamics of benthic-pelagic assemblages in the middle slope of the Balearic Basin (NW Mediterranean). *Deep-Sea Res. I* 61, 84–99.
- Peres-Neto, P.R., Legendre, P., 2010. Estimating and controlling for spatial structure in the study of ecological communities. *Glob. Ecol. Biogeogr.* 9, 174–184.
- R Development Core Team, 2008. *R: A language and environment for statistical computing*.
- Ramirez-Llodra, E., Brandt, A., Danovaro, R., De Mol, B., Escobar, E., German, C.R., Levin, L.A., Martinez Arbizu, P., Menot, L., Buhl-Mortensen, P., Narayanaswamy, B.E., Smith, C.R., Tittensor, D.P., Tyler, P.A., Vanreusel, A., Vecchione, M., 2010. Deep, diverse and definitely different: unique attributes of the world's largest ecosystem. *Biogeosciences* 7, 2851–2899.
- Ruhl, H.A., Smith, K.L., 2004. Shifts in deep-sea community structure linked to climate and food supply. *Science* 305, 513–515.
- Sanchez-Vidal, A., Canals, M., Calafat, A.M., Lastras, G., Pedrosa-Pàmies, R., Menéndez, M., Medina, R., Company, J.B., Hereu, B., Romero, J., Alcoverro, T., 2012. Impacts on the deep-sea ecosystem by a severe coastal storm. *PLoS One* 7, e30395.
- Schurmann, H., Claireaux, G., Chartois, H., 1998. Changes in vertical distribution of sea bass (*Dicentrarchus labrax* L.) during a hypoxic episode. *Hydrobiologia* 371–372, 207–213.
- Sellanes, J., Quiroga, E., Neira, C., Gutierrez, D., 2007. Changes of macrobenthos composition under different ENSO cycle conditions on the continental shelf off central Chile. *Cont. Shelf Res.* 27, 1002–1016.
- Simpson, J.E., 1982. Gravity currents in the laboratory, atmosphere, and ocean. *Ann. Rev. Fluid Mech.* 14, 213–234.
- Sokolove, P.G., Bushell, W.N., 1978. Chi square periodogram: its utility for analysis of circadian rhythms. *J. Theor. Biol.* 72, 131–160.
- Theede, H., 1973. Comparative studies on the influence of oxygen deficiency and hydrogen sulphide on marine bottom invertebrates. *Neth. J. Sea Res.* 7, 244–252.
- Thiel, H., Kirstein, K.O., Luth, C., Luth, U., Luther, G., Meyer-Reil, L.A., Pfannkuche, O., Weydert, M., 1994. Scientific requirements for an abyssal benthic laboratory. *J. Mar. Syst.* 4, 421–439.
- Thistle, D., Ertman, S., Fauchald, K., 1991. The fauna of the Hebble site – Patterns in standing stock and sediment-dynamic effects. *Mar. Geol.* 99, 413–422.
- Thomson, R.E., 1981. *The Oceanography of the British Columbia Coast*. Canadian Special Publication of Fisheries and Aquatic Sciences. Bulletin 56. Fisheries and Oceans, Canada, Ottawa, p. 291.
- Vardaro, M.F., Parmley, D., Smith Jr., K.L., 2007. A study of possible “reef effects” caused by a long-term time-lapse camera in the deep North Pacific. *Deep-Sea Res. I* 54, 1231–1240.
- Wagner, H.-J., Kemp, K., Mattheus, U., Priede, I.G., 2007. Rhythms at the bottom of the deep sea: cyclic current flow changes and melatonin patterns in two species of demersal fish. *Deep-Sea Res. I* 54, 1944–1956.
- Widder, E.A., Robison, B.H., Reisenbichler, K.R., Haddock, S.H.D., 2005. Using red light for *in situ* observations of deep-sea fishes. *Deep-Sea Res. I* 52, 2077–2085.
- Yahel, G., Yahel, R., Katz, T., Lazar, B., Herut, B., Tunnicliffe, V., 2008. Fish activity: a major mechanism for sediment resuspension and organic matter remineralization in coastal marine sediments. *Mar. Ecol. Prog. Ser.* 372, 195–209.